Single-step laser sintering of YSZ powder-beds to TBC applications

V. T. Mazur[1], D. C. Chagas[2,3], M. M. Mazur[4], S. A. Pianaro[4], G. de Vasconcelos[2,3]*

[1]*Federal University of Technology - Parana, UTFPR, 85053-525, Guarapuava, PR, Brazil*
[2]*Aeronautical Institute of Technology, DCTA, 12228-900, São José dos Campos, SP, Brazil*
[3]*Institute for Advanced Studies, DCTA, 12228-001, São José dos Campos, SP, Brazil*
[4]*State University of Ponta Grossa, Av. Carlos Cavalcanti 800, 84010-919, Ponta Grossa, PR, Brazil*

Abstract

Ceramics are widely employed as thermal insulating materials for thermal barrier coatings (TBC) due to their low thermal conductivity, chemical stability, and high wear and corrosion resistance at high temperatures. The aim of this work was to study the influence of the CO_2 laser beam parameters on the single-step irradiation of pre-placed yttria-stabilized zirconia (YSZ) powders on NiCrAlY/AISI 316L substrates. In order to increase the coating's lifetime and performance, it is proposed a laser sintering of powder-beds (LSP) technique to obtain homogenous YSZ coatings, with controlled surface microstructures. The obtained coatings were characterized by optical microscopy, field emission scanning electron microscopy, energy dispersive spectroscopy, and X-ray diffraction (XRD). The laser intensity and interaction time were the main laser parameters used to control the surface temperature and the combination of these parameters were used to establish a process chart. The LSP resulted in controlled smooth coating surfaces and columnar growth with submicrometric grain size. XRD analyses showed the prevalence of non-transformable tetragonal zirconia, which is known to exhibit higher stability and thermal wear resistance.
Keywords: sintering, surfaces, thermal properties, ZrO_2.

INTRODUCTION

Yttria-stabilized zirconia (YSZ) is a well-known material used as a top coat for the three-layer thermal barrier coatings (TBC), employed in high-temperature applications, such as turbine blades for aircraft, diesel internal combustion engines, and others [1]. The other two TBC layers are composed of a bond coat, usually an MCrAlY (M= Ni and/or Co) and a thermally grown oxide (TGO) layer of alumina. Different techniques are industrially employed to deposit the TBC, such as air plasma spray (APS), vacuum plasma spray (VPS), and electron beam physical vapor deposition (EB-PVD), to quote a few. In this field, the published literature is wide and well established. However, these mentioned deposition techniques result in TBC microstructures that can be further improved to increase the TBC lifetime and application temperatures.

Laser technology is a tool that offers different approaches to microstructure development, using powder addition or metal wire methods [2]. 3D parts can be built using laser technology in direct deposition, compositionally graded deposition, additive laser deposition [3], laser powder bed [2], laser cladding, and other techniques. Furthermore, there are recent works in the literature about laser remelting of APS deposition of TBC, with interesting results presenting lifetime increase due to reduction of the density/number and the average size of vertical cracks in the YSZ coating [4]. Wang et al. [5] called laser glazing a promising technique to seal the surface of TBC. YSZ is a permeable material to oxygen ions, which diffuse into the ceramic layer and promote TGO growth. This is known as a mechanism that leads to TBC failure. Ghasemi et al. [6] reported that the laser glazing of YSZ deposited by APS promotes reduction in roughness, leading to higher hot corrosion resistance. The authors performed laser glazing of preheated APS coating, increasing the YSZ density and reducing the grain size and crack density. These characteristics allowed for an increase in toughness and hardness, as well as reducing the stress between substrate and coating. Fan et al. [7] showed that laser glazing promoted a self-healing effect due to the high strain tolerance of cracks exposed to thermal cycling. The laser modification of microstructures was also responsible for delaying crack propagation on the YSZ coating [8]. Following toward the same objective, Wu et al. [9] used an electron beam as a heat source to partially melt an APS YSZ coating under vacuum, obtaining similar results.

The current investigation aims to perform a single-step laser sintering of powder-beds (LSP) to promote the formation of a YSZ coating. The sintering of coatings with the LSP technique makes it possible to obtain in a single step process the aforementioned characteristics, such as increased density, sealing the TBC surface, and reduced roughness. The technique consists of a pre-placed powder bed that has been laser irradiated, promoting powder melting and rapid cooling, leading to the formation of a smooth but cracked high-density YSZ coating with reduced grain size.

MATERIALS AND METHODS

Materials: the current research used the AISI 316L stainless steel (Realum) as substrate material for the

*https://orcid.org/0000-0002-7382-580X

Table I - Chemical composition of AISI 316L (by X-ray fluorescence spectroscopy, Axios Advanced, Panalytical).

Fe	Cr	Ni	Mo	Mn	Si	V	P	Al	Co
68.3	16.98	10.63	2.15	1.43	0.37	0.06	0.04	0.03	0.02

experimental tests with a NiCrAlY layer (Praxair), with a chemical composition consisting of 49.5% Ni, 33% Cr, 11% Al, and 6.5% Y. The AISI 316 L chemical composition is described in Table I. The methodology employed in the LSP of NiCrAlY was previously described elsewhere [10]. The YSZ (ZrO_2 with 8% Y_2O_3) powder (Praxair) was milled in a nylon jar, using 25 g of YSZ balls with a diameter of 1.0±0.1 mm, until it reached particle sizes smaller than 12 μm (1190L, Cilas). 100 g of YSZ powder was mixed with ethyl alcohol. The milling process (PM 100CM, Retsch) was carried out at 500 rpm for 60 min.

YSZ powder pre-deposition: a pneumatic pistol was employed to pre-deposit the YSZ milled powder bed on substrates heated at 70 °C with a thermal blower (HG1100, Makita). The powder thickness, as pre-deposited, was 300±10 μm. Until used, the samples were kept in a drying oven at 50 °C for at least 10 min, to completely evaporate the alcohol.

Laser sintering of powder-bed: during the laser irradiation, argon was used as shielding gas (5 L/min). A continuous Gaussian CO_2 laser device (Evolution 125, Synrad) with maximum power (P) of 125 W was employed as a heat source. The laser quality factor was 1.2 M^2. The laser focalization was performed with a 125 mm lens. Fig. 1

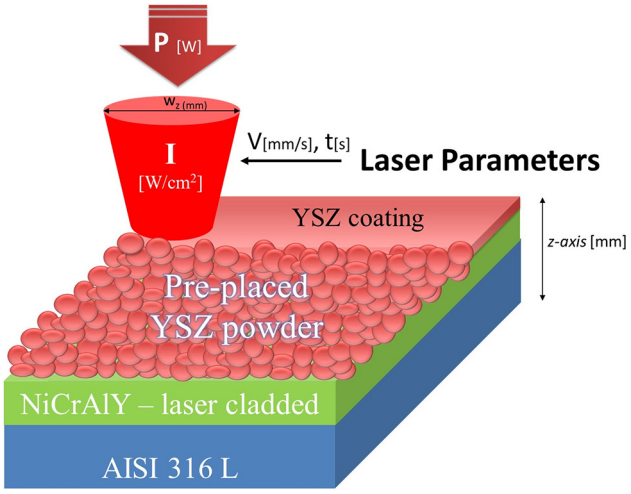

Figure 1: Schematic drawing of laser sintering of powder-beds (LSP) for YSZ.

shows a schematic drawing of the LSP technique. Depending on the desired laser intensity (I) for the experimental trials, the samples were moved on the z-axis to change the laser diameter (w_z), according to the laser propagation equations [11]. According to the changes in z-axis position from the focus position, the overlap was recalculated for each position, maintaining at 70%. The laser irradiation scanning speed (V) was also changed for the experimental trials. The interaction time (t) was calculated according to the ratio w_z/V. Table II shows the set combinations of laser parameters used. The laser power P and overlapping were kept at 125 W and 70% for all experiments. The combinations of beam diameter, intensity, and z-axis positions indicated in Table II were irradiated with eight different scanning speeds: 10, 100, 500, 1000, 2000, 3000, 4000, and 5000 mm/s.

Sample preparation for analysis: after the laser irradiation of YSZ coatings, the sample cross-section was prepared for optical microscopy (Imager.A2m, Zeiss), scanning electron microscopy (SEM, 435 VPi, Leo), and field emission scanning electron microscopy (FEG-SEM, Mira 3, Tescan). The preparation consisted of: grinding (600, 1200#), polishing with alumina (1 and 0.5 μm), etching with an HNO_3-HCl solution for 15 s of immersion, washing in running water, and drying with a thermal blower. The X-ray Bragg Brentano analysis (X'Pert PRO-MPD, Panalytical) was performed on the surface of the sample after cleaning it with acetone in an ultrasound bath. The phases' quantification was determined by the Rietveld method, with GSAS software, according to Assis [12].

RESULTS AND DISCUSSION

The temperature at the surface of the sample is the determining factor for the proper sintering of the YSZ coating. The temperature increase promoted by the laser beam is dictated by the laser intensity and interaction time. In practical terms, temperature control is a function of the z-axis position regarding the laser focus and the scanning speed. Fig. 2 shows surface micrographic images of the obtained coating for laser parameters that characterize four different results or cases: I-detachment, II-complete covering, III-incomplete covering, and IV-unaltered substrate. The micrographs are ordered accordingly to the

Table II - LSP parameters: laser diameter (w_z), laser intensity (I), and z-axis position (z).

w_z (μm)	180.0	180.4	181.4	183.2	185.6	188.7	192.4	196.7	201.6	206.9	212.7	219.0	225.6
I (MW/cm^2)	491.2	489.3	483.5	474.3	461.9	446.9	429.8	411.3	391.8	371.8	351.7	331.9	312.6
z (mm)	0	0.7	1.4	2.1	2.8	3.5	4.2	4.9	5.6	6.3	7.0	7.7	8.4

laser intensity and interaction time parameters (calculated for each beam diameter and scanning speed). The data embedded in the micrographs of Fig. 2 are the result of semi-quantitative elemental analysis performed by energy dispersive spectroscopy (EDS).

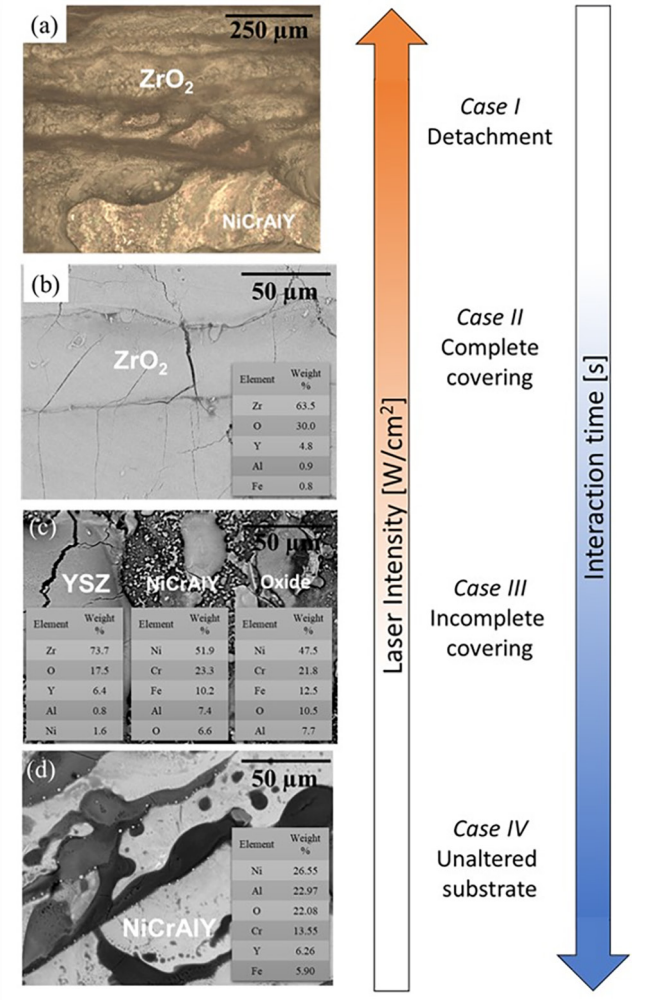

Figure 2: Resulting sintering cases regarding the laser parameters: a) detachment, V=10 mm/s and I=6x10^5 W/cm^2; b) complete covering, V=500 mm/s and I=3x10^6 W/cm^2; c) incomplete covering, V=500 mm/s and I=1x10^5 W/cm^2; and d) unaltered substrate, V=5000 mm/s and I=2.4x10^5 W/cm^2.

Case I - detachment: the detachment of YSZ coating observed in Fig. 2a occurred due to excessive heat accumulation. For low scanning speed (10 mm/s) combined with elevated laser intensity (6x10^5 W/cm^2), the heat accumulation becomes increasingly relevant [13]. The heat dissipation occurs at a low rate, causing the coating to partially vaporize, changing the stoichiometry of components and ultimately promoting detachment, as observed in the optical micrograph of Fig. 2a, where the underlying NiCrAlY layer is exposed and can even be observed at low magnification.

Case II - complete covering: Fig. 2b shows the SEM micrograph of an optimized situation for the coating sintering. It can be observed that a cracked but homogenous layer of YSZ was obtained. Horizontal lines were the result of successive and adjacent laser tracks, which were performed with 70% overlap. According to the literature studies, a high strain tolerance can be achieved with the formation of vertical cracks [7].

Case III - incomplete covering: when the temperature was below the threshold for complete melting and sintering throughout the surface, isolated islands of YSZ were obtained. Although the sintering was incomplete, the temperature was high enough to produce microstructural changes on the NiCrAlY layer, with the formation of plate-like oxide structures, as indicated in the SEM micrograph of Fig. 2c. Given the cases I and III as indicative, a process window was found, where complete covering was outlined to maximize the process energy efficiency, making it possible to achieve the highest scanning speed with the lowest laser intensity.

Case IV - unaltered substrate: with insufficient temperature, no changes were observed in the SEM micrograph of the NiCrAlY layer. The YSZ powder was removed by simple cleaning after the laser irradiation.

These behaviors were observed for different combinations of intensity and scanning speed or interaction time. Fixing the scanning speed and gradually setting the laser intensity allowed the compilation of data to create a graphical process chart, as can be seen in Fig. 3. Due to the employed equipment limitations, the scanning speed was adjusted from 10 to 5000 mm/s. The same methodology can be applied to determine process charts for different types of coatings, with different powder bed thicknesses.

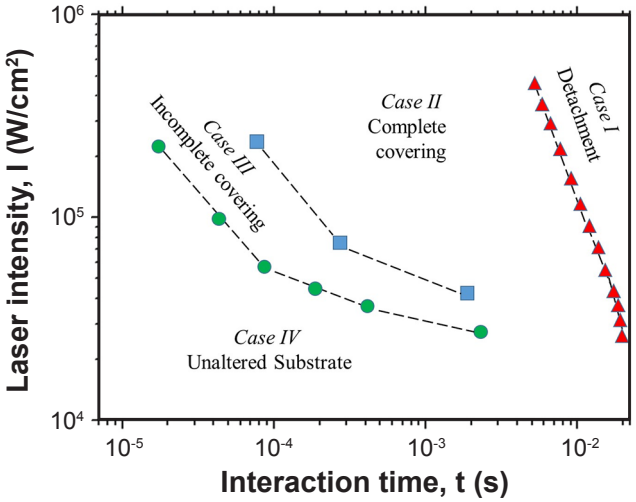

Figure 3: Process chart for the LSP for yttrium-stabilized zirconia as a function of laser intensity and interaction time (t=2w$_z$/V), calculated as laser beam diameter per scanning speed.

Phase composition and microstructure: further characterizations were carried out on case II (complete covering) samples. Fig. 4 shows the X-ray diffraction pattern for the laser-sintered YSZ coating in comparison with the as-received YSZ powder material. Different zirconia crystalline structures were present in the powder

material: monoclinic (m), cubic (c), and transformable tetragonal (t). After the laser irradiation, the predominance was the non-transformable tetragonal (t'). Similar results were reported by Ghasemi et al. [6] and Fan et al. [7] for laser modification of YSZ previously deposited by APS. A Rietveld quantitative estimation of phases is presented in Table III. It was observed that even with high rates of cooling due to the laser processing, cubic and transformable phases of zirconia still remained, although, it is important to highlight that the prevalence phase was t'. This phase is interesting for applications above 800 °C, presenting higher stability and thermal resistance than the other phases.

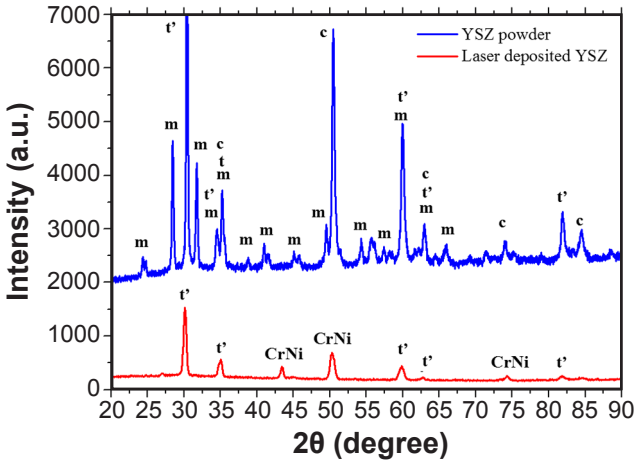

Figure 4: X-ray diffraction patterns for as-received zirconia powder and after the LSP, showing the zirconia phases: m: monoclinic, c: cubic, t: tetragonal, and t': non-transformable tetragonal.

Table III - Quantitative Rietveld analysis of laser deposited YSZ.

Phase	Content (%)
Non-transformable zirconia, t'-ZrO_2	72.84
Transformable tetragonal zirconia, t-ZrO_2	6.29
Cubic zirconia, c-ZrO_2	20.87

Regarding the coating microstructure, Fig. 5a shows an SEM micrograph, where the sample was tilted, providing the observation of the cross-section and the coating surface. On the surface, there was an interface generated by the laser overlap, where a remarkable difference in the grain boundaries was present. Figs. 5b and 5c are FEG-SEM micrographs showing the grain boundaries. A smoothening in the overlap region was observed. This can be explained by the changes in the optical properties of the material and the manner in which the laser irradiation interacted with it. According to Pecharromán et al. [14], the absorption by a matter of the infrared light produced by the CO_2 laser is determined not only by its chemical composition and structure but also by the shape of the powder particles and aggregation state when comprising the powder bed. The first track used the available energy to promote the powder melting to form the coating. However, in the overlapping region, the energy remelted the previously formed track, changing the microstructure, where the grain boundaries were no longer distinguishable, with the surface becoming smoothened [15].

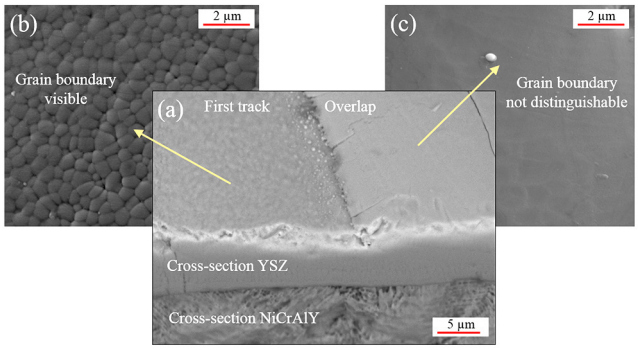

Figure 5: SEM micrograph of a prepared cross-section (a) and FEG-SEM micrographs with higher magnification of the laser-sintered YSZ coating of the indicated regions (b,c).

In order to investigate the internal structure, a fracture analysis by FEG-SEM was carried out, as shown in Fig. 6. A columnar growth is observed in Fig. 6a, which comprises the region where the grain boundaries were visible. The same behavior is observed for Fig. 6b, where an indistinguishable grain boundary was present. This indicated that even with track overlapping, the inner columnar microstructure was preserved. The average grain size observed was 0.7±0.2 µm. Small grain sizes increase the coating hardness [5]. It has been established that laser overlap is an important parameter to determine the surface microstructural characteristics of the YSZ coating. Increasing the overlap could promote surface smoothing, as indicated by the current investigation results. Further investigations must be conducted to elucidate how multiple irradiation cycles could change the surface smoothness. According to literature studies [5, 6], smoothened surfaces may present a higher lifetime by reducing the penetration of oxidizing ions or salts through the YSZ coating especially at high temperatures during operation.

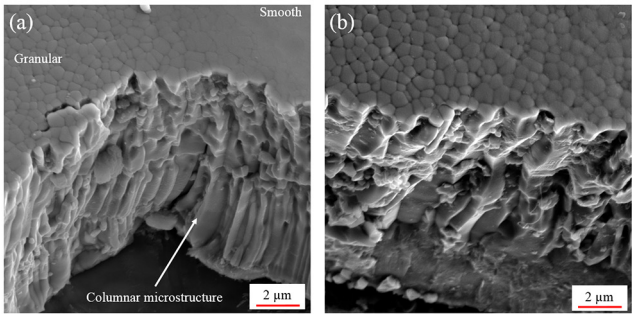

Figure 6: FEG-SEM images of fractured YSZ coating showing regions where grain boundaries are: a) visible; and b) indistinguishable.

CONCLUSIONS

An experimental process chart for the laser sintering of yttria-stabilized zirconia (YSZ) coating from a pre-deposited powder bed of 300 μm was developed focusing on the laser parameters: laser intensity and scanning speed. Excessive laser intensity or interaction time can cause the coating to detach during the process, while shorter interaction time or intensity does not promote homogeneous covering. Once the sintering threshold is established, the laser overlap can be adjusted to produce rough or smooth coating surfaces. Furthermore, the YSZ coating shows columnar growth, with submicrometric grain size, regardless of the laser overlap. X-ray diffraction analysis demonstrated the prevalence of non-transformable tetragonal zirconia, which is preferable for applications above 800 °C due to higher stability and thermal wear resistance.

ACKNOWLEDGMENTS

The authors acknowledge CNPq/MCT/AEB (National Research Council/Science and Technology Ministry/ Brazilian Space Agency), FAPESP (Research Foundation of the São Paulo State - process nº 2013/08920-1), AMR-DCTA (Materials Division - Aerospace Technology and Science Department), LAS-INPE (Associate Laboratory of Sensors and Materials - National Institute for Space Research), CLABMU - UEPG (Complex Multi-User Laboratories - State University of Ponta Grossa), and Rafael Teleginski for review.

REFERENCES

[1] A. Thibblin, S. Jonsson, U. Olofsson, Surf. Coat. Technol. **350** (2018) 1.
[2] R. Vilar, Comp. Mater. Proc. **10** (2014) 163.
[3] U. Savitha, V. Srinivas, G.J. Reddy, A.A. Gokhale, M. Sundararaman, Surf. Coat. Technol. **354** (2018) 257.
[4] C. Zhao, M. Zhao, M. Shahid, M. Wang, W. Pan, Surf. Coat. Technol. **309** (2017) 1119.
[5] Y. Wang, G. Darut, X.-T. Luo, T. Poirier, J. Stella, H. Liao, M.-P. Planche, Ceram. Int. **43** (2017) 4606.
[6] R. Ghasemi, R. Shoja-Razavi, R. Mozafarinia, H. Jamali, M. Hajizadeh-Oghaz, R. Ahmadi-Pidani, J. Eur. Ceram. Soc. **34** (2014) 2013.
[7] Z. Fan, K. Wang, X. Dong, W. Duan, R. Wang, X. Mei, W. Wang, J. Cui, S. Zhang, C. Xu, Mater. Lett. **188** (2017) 145.
[8] F. Chang, K. Zhou, X. Tong, L. Xu, X. Zhang, M. Liu, Appl. Surf. Sci. **317** (2014) 598.
[9] Y.-Z. Wu, W.-B. Liao, F. Wang, M.-L. Wang, C.-Y. Yu, Z. Wang, Z.-X. Guo, Z.-Y. Liu, Y.-B. Cao, J.-J. Huang, J. Alloys Compd. **756** (2018) 33.
[10] V. Teleginski, D.C. Chagas, L.G. Oliveira, G. Vasconcelos, Mater. Sci. Forum **802** (2014) 409.
[11] WM. Steen, J. Mazumder, *Laser material processing*, 4th ed., Springer, London (2010).
[12] JMK. Assis, "Crystalline phases stabilization study of ceramics of the niobia-yttria-zirconia system", Doct. Thesis, Inst. Nac. Pesq. Espac. (2014).
[13] J. Finger, M. Reininghaus, Opt. Express **22** (2014) 18790.
[14] C. Pecharromán, M. Ocaña, C.J. Serna, J. Appl. Phys. **80** (1996) 3479.
[15] V. Teleginski, "Deposição de revestimentos com laser de CO_2 para proteção térmica de palhetas de turbinas aeronáuticas e industriais", Doct. Thesis, Inst. Tecn. Aeronáut. (2016).
(Rec. 23/11/2020, Rev. 28/02/2021, 07/04/2021, Ac. 12/04/2021)